

# TH<sub>z</sub> transmission resonances in metalized and defect photonic structures for precise optical monitoring

## Abstract

A photonic crystal resonator optically contacted with a metal film generates in the THz frequency range a system of sharp spikes of electromagnetic quenching matching the reflection spectra of bare resonator. In this work, we found that sharp spikes of electromagnetic transmission can also be generated at certain conditions by the defect containing resonators. The sharp needle like angle and frequency dependence of spikes induced by metal or defect can serve as a ground effect in compact and reliable direction control devices and THz radiation collimating devices.

**Keywords:** photonic crystal, planar layered structure, light reflection spectroscopy, bandgap structure, local states, spike lines of transmission, precise pressure measurement optical devices

Volume 7 Issue 1 - 2021

**E Ya Glushko**

Department of Semiconductor Photonic Structures, Institute of Semiconductor Physics of NAS of Ukraine, Ukraine

**Correspondence:** E Ya Glushko, Department of Semiconductor Photonic Structures, Institute of Semiconductor Physics of NAS of Ukraine, Nauki Prsp 41, 03028, Kyiv, Ukraine, Tel +038 044 525 2309, Email scientist.com\_eugene.glushko@mail.com

**Received:** October 31, 2020 | **Published:** January 05, 2021

**Abbreviations:** PhCr, photonic crystal; OPM, opto-pneumatic medium; EMF, electromagnetic field; TIR, total internal reflection; SP, surface plasmon; PP, polypropylene; HWHM, half width on half maximum

## Introduction

Last decades, the THz photonics have become a quickly developing area with wide spectrum of applications in different domains. A huge base of technologies and investigation methods is concentrated in this field.<sup>1-4</sup> In biology and medicine, the THz range of frequencies provides soft and harmless instruments for aims of sensing and imaging.<sup>2,3,5,6</sup> The PhCr structures in this regard, are of a great interest due to their useful technological properties. The ordered photonic structures are used in optical technologies to create perfect dielectric mirrors, high-performance optical filters, and a lot of other applications were developed. It worth noting that dominating properties attracting attention are the existing omnidirection reflection windows and a possibility to create integrated waveguide structures in 2D and 1D PhCr. In,<sup>7</sup> a new scheme of realizing terahertz fingerprint detection with ultrahigh sensitivity was proposed using a cavity mode resonating at the characteristic frequency of the sample. Also, the position of reflection window edge may be sensitive to external conditions that is used in the so-called optopneumatic media (OPM). The gas-filled SiO<sub>2</sub>/air OPM structure as an element of a compact all-optical device were analysed in<sup>8</sup> to indicate pressure over time inside the fluid flow. Besides, the OPM can be used in the high-accuracy measurement procedure for the universal gas constant.<sup>9</sup> Recently new interesting phenomena promising useful applications were found in metalized planar PhCr in the THz range.<sup>10</sup> In this study, we concentrate on the important role of extremely sharp reflection and transmission resonances which can be useful sensitive markers of state of the art in media under investigation.

## Spikes of quenching in a metalized photonic resonator

In the terahertz frequency range, a polarized electromagnetic wave (EMW) interacting with a metal film through a planar photonic

crystal resonator region exhibits some unusual forms of reflection and transmission. The physical nature of arising effects can be explained by extremely high both real and imaginary parts of refraction index of metals in the THz region of frequencies. We have investigated theoretically a correlation between spectra of a bare photonic structure and that deposited on a gold film (Figure 1). The frequency dependent complex refractive index of Au in the terahertz frequency range was measured in.<sup>11</sup> Here we use a convenient analytical approximation for gold electric permittivity proposed in.<sup>9</sup> It was found there that for quasi-normal incidence of EMW the presence of metal generates narrow spectral wells in the middle of reflection windows existing for the same free photonic crystal. An investigation of properties including the resonances shape showed that they are of Fano type. Quite another manifestation of metal-resonator inter-influence takes place at whispering incident angles when reflection spikes of a p-polarized wave coincide with modes of photonic crystal resonator and they are absent throughout the stop band areas between modes. This behaviour is typical for a surface plasmon (SP) resonance. The effect is strongly depended on polarization, number of periods and angle of incidence. The s-polarized field exhibits more complicate features: at whispering incident angles the resonances in vicinity of low energy modes of each band arise between them (Fano type resonances) whereas the resonances with higher energy close to the top of band became to be matched the mode frequencies (SP resonances).

In Figure 2, shown is the calculated diagram of reflection in geometry 5, 6 (Figure 1) for a 8-period PP/air photonic crystal contacting a 40 nm gold film. The PP layers with thickness  $d_1=200 \mu\text{m}$  are divided by the  $d_2=600 \mu\text{m}$  air voids. Due to the presence of metal, a system of deep and narrow lengthy hollows arises onto the map of reflection matching the middle of reflection windows of the bare PhCr.<sup>9</sup> Both p-and-s-polarizations give for incident angles less than 45° three spike lines of transmission inside the considered interval of frequencies (0, 800) GHz. The spikes position and shape depend on the resonator parameters. For instance, the maximal depth ( $R=0$ ) of the second spike  $v_2$  (328.10 GHz, Figure 2A) is reached at  $N=11$  with HWHM=0.06 GHz, the maximal quenching is moved to higher  $N$  for the next number spikes. The spike  $v_3$  (683.10 GHz) becomes

maximally deep at  $N=13$  with HWHM=0.08 GHz. The width at the half maximum of spike decreases with the growth of metal film thickness and reaches for this spike HWHM=0.02 GHz at  $d_m=180$  nm. In Figure 2A & 2B, also shown are the difference in positions of reflection spikes for different polarizations at whispering incidence. A vertical section at a chosen frequency in lower parts of Figure 2A & 2B gives the angle dependence of reflection. In a metalized resonator, the angular width of spike lines is essentially narrowing. For the spike  $v_z$  at 350 GHz and  $d_m=40$  nm the HWHM is about 0.4° and decreases with the growth of metal film thickness  $d_m$  what opens a possibility to collimate divergent electromagnetic beam transmitting through the system. A comparison of results for different metals shows that the spike position is practically independent on the adopted model of metal. In general, a metal with higher conductivity “eats” a deeper hole in the curve of reflection at the same position of spike’s tip.

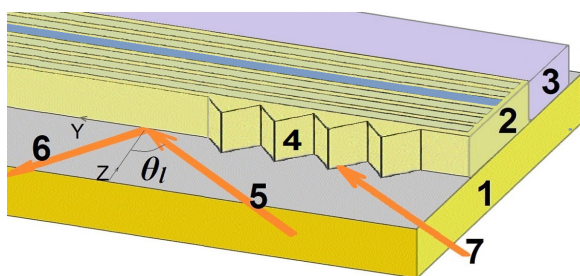


**Figure 1** A planar layered defect photonic crystal resonator contacting with a metal. 1, substrate; 2, 5-period photonic crystal with a highlighted defect layer; 3, metal film, 4, input prism, 5, 6, incident and reflected beams in external geometry of incidence, 7,  $\theta_I$ , incident angle.

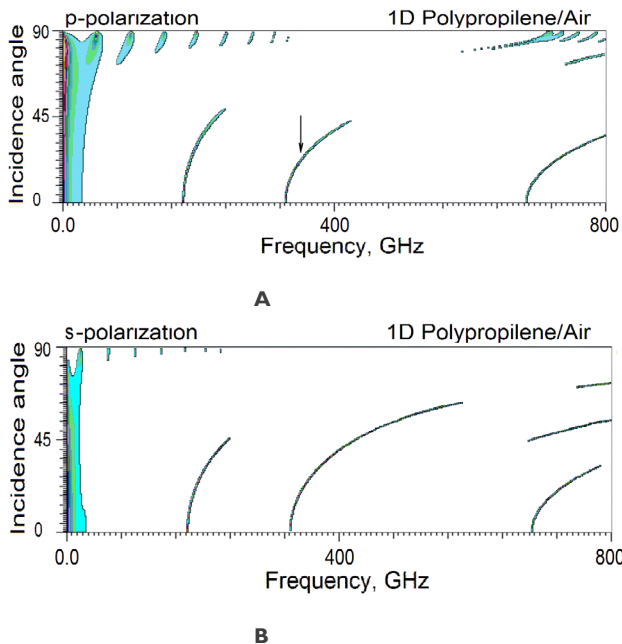


**Figure 2** Reflection map of an 8-period PP/air photonic crystal contacting the gold film  $d_m=40$  nm in geometry 5, 6.  $d_1=200$   $\mu$ m,  $d_2=600$   $\mu$ m. (A) p-polarization. Arrow, 350 GHz. (B) s-polarization.

### Spikes of transmission in a defect contained photonic resonator

We have also considered the PhCr structure containing an inserted defect layer (Figure 1, highlighted layer). Following<sup>9</sup> we calculated

the photonic band gap structure existing inside the TIR angle region  $\theta_I \in (17^\circ, 90^\circ)$  of a 10 period (Si/PP)<sub>5</sub>D(Si/PP)<sub>5</sub> resonator, where  $\theta_I$  is the incident angle inside the Si layers. The defect layer D is situated in the middle of structure. Due to the transparency of Si in the THz range under consideration,<sup>12,13</sup> a possibility to create resonators with high intrinsic optical contrast arises. The high enough optical contrast of the PhCr is a condition of local and surface states existence. In Figure 3 (upper panel), the calculated mode structure is presented for geometry 7 (Figure 1) when standing eigenmodes can be excited in the TIR region of the resonator. The Si layers of the PhCr  $d_1=300$   $\mu$ m are divided by the PP layers  $d_2=1000$   $\mu$ m. The thickness of silicon defect layer D  $d_d$  was chosen 300  $\mu$ m. If  $d_d \rightarrow 0$  then only surface states exist. Beginning with  $d_d \approx 84$   $\mu$ m an intrinsic local state  $v_d \approx 75.8$  GHz arises with density of field concentrated near the layer D. When the thickness reaches  $d_d=300$   $\mu$ m, the local state frequency in vicinity of TIR angle 17° shifts from 75.8 GHz to the long wavelength side and occupies position  $v_d=73.8$  GHz. Our evaluations show a complicated behaviour of the local mode depending on geometrical sizes. In Figure 3 (lower panel), the reflection map of a defect contained structure in geometry 5, 6 is shown for the frequency interval (50, 110) GHz. The presence of defect layer D generates a narrow lengthy line of perfect transmission beginning with normal incidence and up to whispering angles of incidence.

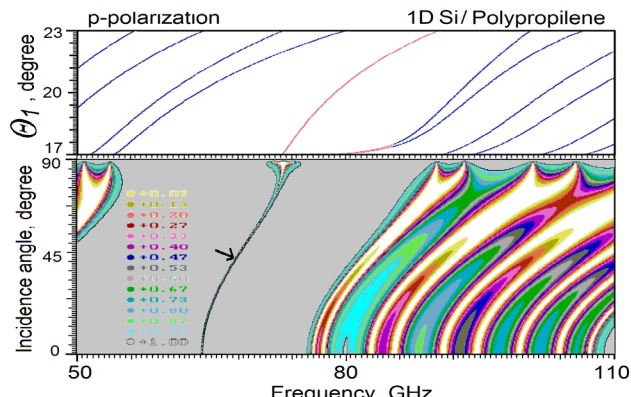


**Figure 3** Mode spectrum and reflection map of the (Si/PP)<sub>5</sub>Si(Si/PP)<sub>5</sub> photonic crystal containing a defect layer  $d_d=300$   $\mu$ m. Silicon layer thickness  $d_1=300$   $\mu$ m, polypropylene layer thickness  $d_2=1000$   $\mu$ m, p-polarization. Upper panel: Bandgap structure in interval  $\theta_I \in (17^\circ, 23^\circ)$  of the TIR region. Defect local state is located in vicinity of the center of gap. Two surface states detached from the second band at  $\theta_I < 17.6^\circ$  once again join the band near  $\theta_I = 17.6^\circ$ . Lower panel: Reflection map of the (Si/PP)<sub>5</sub>Si(Si/PP)<sub>5</sub> photonic crystal. Arrow shows the transmission spike. Inset: 16 step color scale of reflection.

### Energy concentration and collimation effect in a metalized resonator structure

The found feature both of metalized resonators and defect containing resonators to form extremely sharp peaks of transmission can be used to control the divergence of the incident beam. To illustrate how one can collimate a monochromatic diverging irradiation we shall consider a stochastic EMW reservoir which can to filter and accumulate inside the electromagnetic energy from a source at fixed frequency or fixed angle of incidence. Due to stochastic inner reflection the angle distribution of irradiation inside the reservoir can be treated as close to white noise type. When the average density of energy inside the box reaches its saturation a stable energy flow through the resonator window is established. The flow outside

the EMW reservoir is determined by the accumulated density of electromagnetic energy inside the reservoir. Taking into consideration possible channels of energy leakage and geometrical parameters we found the characteristic time of the process of energy accumulation which depends on the input and output sections of the resonator. For the chosen frequency  $\nu_r = 350 \text{ GHz}$  (shown by arrow in Figure 3A) and volume of the EMW reservoir an essential collimation effect of THz radiation was found with divergence close to  $0.4^\circ$ .

## Conclusion

In conclusion, it was found that both interaction with metal and presence of a defect inside the PhCr generates a system of sharp needle-like areas with quenching of electromagnetic field or, in the case of a defect; it is a spike of perfect transmission. The effect can be treated as a kind of resonant cancellation of reflection in a metalized or defect containing PhCr system. One of the reasons for the sharp resonances in a metalized resonator is extremely high components of refraction index of metals in THz range of frequencies. The induced by a defect or metal film sharp angular and frequency dependence of spikes found here can serve as a ground effect in compact and reliable direction control devices and THz radiation collimating devices.

## Acknowledgments

None.

## Conflicts of interest

The author declares that there is no conflict of interest.

## References

1. Dragoman D, Dragoman M. Terahertz fields and applications. *Prog Quant Electron*. 2004;28:1–66.
2. Dhillon SS, Vitiello MS, Linfield EH, et al. The 2017 terahertz science and technology roadmap. *J Phys D: Appl Phys*. 2017;50:043001.
3. Sizov FF. Infrared and terahertz in biomedicine emiconductor. *Physics Quantum Electronics & Optoelectronics*. 2017;20:273–283.
4. Xia J, Qiao Q, Zhou G, et al. Opto-Mechanical Photonic Crystal Cavities for Sensing Application. *Appl Sci*. 2010;10:7080.
5. Pickwell E, Wallace VP. Biomedical applications of terahertz technology. *J Phys D Appl Phys*. 2006;39:R301–R310.
6. Danciu M, Alexa-Stratulat T, Stefanescu C. Terahertz spectroscopy and imaging: a cutting-edge method for diagnosing digestive cancers. *Materials*. 2019;12:1519.
7. Shi X, Han Zh. Enhanced terahertz fingerprint detection with ultrahigh sensitivity using the cavity defect modes. *Scientific Reports*. 2017;7:13147.
8. Glushko EY, Stepanyuk AN. A pneumatic photonic structure: precise optical indication of pressure over time inside the fluid flow. *Int J Biosen Bioelectron*. 2018;4(3):109–112.
9. Glushko EY. Based on pneumatic photonic structures, high-accuracy measurement procedure for the universal gas constant, Nanophotonics, Nano optics, Nanobiotechnology, and Their Applications. *Springer Proceedings in Physics*. 2019;222:103–120.
10. Glushko EY. Mixed Fano-SP resonant absorption of THz electromagnetic waves in a photonic resonator contacting with a metal film. *Physics Letters A*. 2020;384(23):126564.
11. Yasuda H, Hosako I. Measurement of Terahertz Refractive Index of Metal with Terahertz Time-Domain Spectroscopy. *Jpn J Appl Phys*. 2008;47:1632–1634.
12. Exter M, Grischkowsky D. Optical and electronic properties of doped silicon from 0.1 to 2 THz. *Applied Physics Letters*. 1990;56(17):1694–1696.
13. Sanjuan F, Tocho JO. Optical properties of silicon, sapphire, silica and glass in the Terahertz range. Latin America Optics and Photonics Conference, paper LT4C.1. 2012.